Rsd balances (p)ppGpp level by stimulating the hydrolase activity of SpoT during carbon source downshift in *Escherichia coli*

Jae-Woo Lee[1†], Young-Ha Park[2†], Yeong-Jae Seok[1,2*]

[1]Department of Biophysics and Chemical Biology, Seoul National University, Seoul 08826, Republic of Korea

[2]School of Biological Sciences and Institute of Microbiology, Seoul National University, Seoul 08826, Republic of Korea

[†]These authors equally contributed to this work.

[*]Corresponding author: Tel: 82-2-880-8827; E-mail: yjseok@snu.ac.kr

Supporting Information

Tables S1 and S2

Figures S1 – S10

Supplementary references

www.pnas.org/cgi/doi/10.1073/pnas.1722514115

Table S1. Bacterial strains and plasmids used in this study

Strain or plasmid	Genotype or phenotype	Source
Strains		
MG1655	WT *E. coli* K-12	(1)
ER2566	F⁻ λ⁻ f*huA2* [*lon*] *ompT lacZ::T7 gene 1 gal sulA11* Δ(*mcrC-mrr*)*114::IS10 R*(*mcr-73::miniTn10-TetS*)*2 R*(*zgb-210::Tn10*)(*TetS*) *endA1* [*dcm*]	New England Biolabs
BTH101	F⁻, *cya-99*, *araD139*, *galE15*, *galK16*, *rpsL1* (Str^R), *hsdR2*, *mcrA1*, *mcrB1*	(2)
MG1655Δ*rsd*	MG1655 *rsd*::Tet^R	(3)
MG1655Δ*relA*Δ*spoT*	MG1655 *relA*::Km^R, *spoT*::Cm^R	This study
MG1655Δ*relA*	MG1655 *relA*::Km^R	This study
MG1655Δ*relA*Δ*rsd*	MG1655 *relA*::Km^R, *rsd*::tet^R	This study
GI698	F⁻ λ⁻ *lacI*^{q} *lacPL8 ampC*::P_{trp} cI	(4)
Plasmids		
pETDuet-1	Cloning vector; Amp^R	Novagen
pET-HisRsd	pETDuet-1–derived expression vector for His-Rsd	(3)
pET-Rsd	pETDuet-1–derived expression vector for Rsd	(3)
pET-SpoTC1	pETDuet-1–derived expression vector for truncated version of SpoT (384-702)	This study
pET-SpoTN2	pETDuet-1–derived expression vector for truncated version of SpoT (1-447)	This study
pUT18C	ColEI-ori, P_{lac}::*cyaA* 225–399, encoding *B. pertussis* CyaA T18 fragment, Amp^R	(5)
pUT18C-zip	ColEI-ori, P_{lac}::*cyaA* 225–399φGCN4-zip, Amp^R	(6)
pUT18C-Rsd	Contains *E. coli* Rsd fused to *B. pertussis* CyaA T18 fragment, Amp^R	This study
pUT18C-Rsd(D63A)	Asp63 was mutated to Ala in pUT18C-Rsd	This study
pUT18C-SpoT	Contains *E. coli* SpoT fused to *B. pertussis* CyaA T18 fragment, Amp^R	This study
pKT25	ori p15A, P_{lac}::*cyaA* 1–224, encoding *B. pertussis* CyaA T25 fragment, Km^R	(5)
pKT25-zip	ori p15A, P_{lac}::*cyaA* 1–224φGCN4-zip, Km^R	(7)
pKT25-Rsd	Contains *E. coli* Rsd fused to *B. pertussis* CyaA T25 fragment, Km^R	This study
pKT25-SpoT	Contains *E. coli* SpoT fused to *B. pertussis* CyaA T25 fragment, Km^R	This study
pKT25-SpoTN1	Contains *E. coli* SpoT (1-347) fused to *B. pertussis* CyaA T25 fragment, Km^R	This study
pKT25-SpoTC1	Contains *E. coli* SpoT (384-702) fused to *B. pertussis* CyaA T25 fragment, Km^R	This study
pKT25-SpoTN2	Contains *E. coli* SpoT (1-447) fused to *B. pertussis* CyaA T25 fragment, Km^R	This study
pKT25-SpoTC2	Contains *E. coli* SpoT (448-702) fused to *B. pertussis* CyaA T25 fragment, Km^R	This study
pKT25-RelA	Contains *E. coli* RelA fused to *B. pertussis* CyaA T25 fragment, Km^R	This study
pKT25-EIIA^{Ntr}	Contains *E. coli* EIIA^{Ntr} fused to *B. pertussis* CyaA T25 fragment, Km^R	Gift from CR Lee
pKT25-EIIA^{Ntr}(H73A)	His73 was mutated to Ala in pKT25-EIIA^{Ntr}	Gift from CR Lee

pKT25-EIIA^{Ntr}(H73E)	His73 was mutated to Glu in pKT25-EIIA^{Ntr}	Gift from CR Lee
pGEX-4T-1	Cloning vector; Amp^{R}	GE Healthcare
pGEX-SpoT	pGEX-4T-1–derived expression vector for GST-SpoT	This study
pJK1113	pBAD24 with *oriT* of RP4 and *nptI*, P_{BAD}; Km^{R}, Amp^{R}	(8)
pJK1113-Rsd	pJK1113-derived expression vector for Rsd, Km^{R}, Amp^{R}	This study
pJK1113-HPr(H15A)	pJK1113-derived expression vector for HPr (His15 to Ala), Km^{R}, Cm^{R}	This study
pKD46	Red recombinase expression plasmid under the control of arabinose inducible promoter	(9)
pRE1	Expression vector under control of λP_L promoter, Amp^{R}	(10)
pRE-HisEIIA^{Ntr}	pRE1-based expression vector for His-EIIA^{Ntr}	(11)
pRE-HIcrr	pRE1-based expression vector for HPr, EI and EIIA^{Glc}	(12)
pACYC184	A low copy number cloning vector; Cm^{R} Tet^{R}	(13)
pACYC-HPr	*E. coli ptsH* promoter and its ORF cloned between SphI and SalI sites of pACYC184	(12)
pACYC-Rsd	*E. coli rsd* promoter and its ORF cloned between BamHI and SphI sites of pACYC184	(3)
pACYC-Rsd(D63A)	Asp63 was mutated to Ala in pACYC-Rsd	This study

Table S2. Oligonucleotides used in this study

Name	Oligonucleotide sequence (5'-3')	Use(s)
RS925	AGTTCGCATATGGAATTTATCGAGAGCGTTAAATC (NdeI)	Construction of pET-SpoTC1
RS926	GTTCATAAACTCGAGATTTCGGTTTCGGGTGAC (XhoI)	
RS927	AGCGGGCCATGGCCTTGTATCTGTTTGAAAGCCTG (NcoI)	Construction of pET-SpoTN2
RS928	CGACAAAGAATTCTTACCAAGCGGCATTCGGGCGA (EcoRI)	
RS929	ACAAACTTGCGGAGGATCCCATGCTTAACC (BamHI)	Construction of pUT18C-Rsd
RS930	CTGCGCTGTTAAGAATTCATTTACATTCAA (EcoRI)	
RS931	TTGTCAGAGCCTGGTCGCTTACTTGTCTGCCGGAC	Construction of pUT18C-Rsd(D63A)
RS932	GTCCGGCAGACAAGTAAGCGACCAGGCTCTGACAA	
RS933	CAAAGCGGGGATCCCTTGTATCTGTTTGAAAGCCT (BamHI)	Construction of pUT18C-SpoT
RS934	CCCAACACGTTATGCACGCATGAATTCAATGCTCG (EcoRI)	
RS935	ACAAACTTGCGGAGGATCCCATGCTTAACC (BamHI)	Construction of pKT25-Rsd
RS936	CTGCGCTGTTAAGAATTCATTTACATTCAA (EcoRI)	
RS937	CAAAGCGGGGATCCCTTGTATCTGTTTGAAAGCCT (BamHI)	Construction of pKT25-SpoT
RS938	CCCAACACGTTATGCACGCATGAATTCAATGCTCG (EcoRI)	
RS939	AGCGGGGGATCCATTGTATCTGTTTGAAAGCCTG (BamHI)	Construction of pKT25-SpoTN1
RS940	ATTTGTGAATTCGTACTTTAGGTTTCGCCGTGCTC (EcoRI)	
RS941	GATCTCGGATCCATTCCCGGATGAGATTTACG (BamHI)	Construction of pKT25-SpoTC1
RS942	GTTCATGAATTCTTAATTTCGGTTTCGGGTGAC (EcoRI)	
RS943	AGCGGGGGATCCATTGTATCTGTTTGAAAGCCTG (BamHI)	Construction of pKT25-SpoTN2
RS944	AGCGCCGAATTCTTAGGTAATGATTTCAACGGTT (EcoRI)	
RS945	GAAATCGGATCCAGCTCCGGGCGCTCGCCCGAATG (BamHI)	Construction of pKT25-SpoTC2
RS946	GTTCATGAATTCTTAATTTCGGTTTCGGGTGAC (EcoRI)	
RS947	AAGGAGGGATCCAATGGTTGCGGTAAGAAGTGCAC (BamHI)	Construction of pKT25-RelA
RS948	GCAAATGAATTCCTAACTCCCGTGCAACCGACGCG (EcoRI)	
RS949	AGCGGGGGATCCTTGTATCTGTTTGAAAGCCTG (BamHI)	Construction of pGEX-SpoT
RS950	GTTCATCTCGAGTTAATTTCGGTTTCGGG (XhoI)	
RS951	GCGGAGGAATTCATGCTTAACCAGCTCG (EcoRI)	Construction of pJK1113-Rsd
RS952	ACAGCGGTCGACTCAAGCAGGATGTTTGACGC (SalI)	
RS953	AATACAGTCGACATGTTCCAGCAAGAAGTTACC (SalI)	Construction of pJK1113-HPr(H15A)
RS954	GGGAAAGTCGACTTACTCGAGTTCCGCCATC (SalI)	
RS955	TTGTCAGAGCCTGGTCGCTTACTTGTCTGCCGGAC	Construction of pACYC-Rsd(D63A)
RS956	GTCCGGCAGACAAGTAAGCGACCAGGCTCTGACAA	
SpoT-F	GCCACCTACCAGGATATGGA	qRT-PCR
SpoT-R	GTACGGTCGGCAAGTTTGAT	
RelA-F	GAAGATGTGCTGCGTGAGAG	
RelA-R	GTACACGTTCATCTTCCGGC	

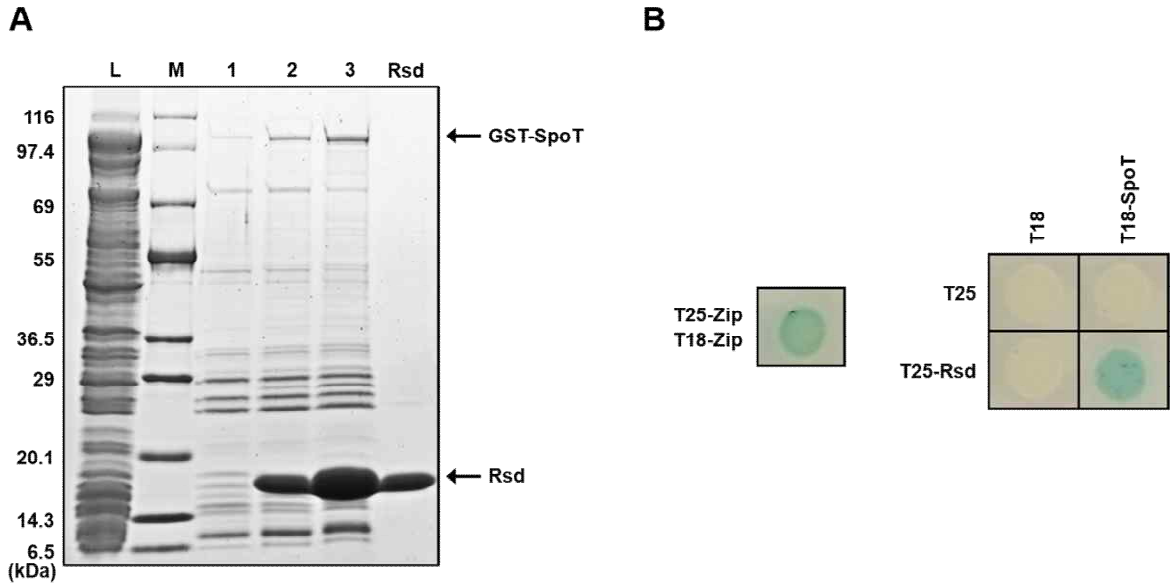

Fig. S1. *In vitro* and *in vivo* interaction of Rsd with SpoT. (*A*) *E. coli* cell extract expressing GST-SpoT was mixed with various amounts of purified Rsd (0, 120, and 360 μg in lanes 1-3, respectively), and each mixture was incubated with 50 μl of TALON resin for metal affinity chromatography. Proteins bound to the resin were eluted with 2x SDS loading buffer (70 μl) and analyzed by SDS-PAGE and stained with Coomassie brilliant blue. Lane L, the *E. coli* cell lysate expressing GST-SpoT; lane M, the molecular mass markers (KOMA Biotech). (*B*) The bacterial two-hybrid (BACTH) assays to analyze the specific interaction of Rsd with SpoT *in vivo*. *E. coli* strain BTH101 coexpressing the indicated proteins was spotted on LB agar plates supplemented with 40 μg/ml X-gal as the color indicator for β-galactosidase activity and incubated at 30°C overnight. Zip, the leucine zipper of *Saccharomyces cerevisiae* GCN4, served as a positive control. The transformant coexpressing the unfused T25- and T18-fragments themselves served as a negative control.

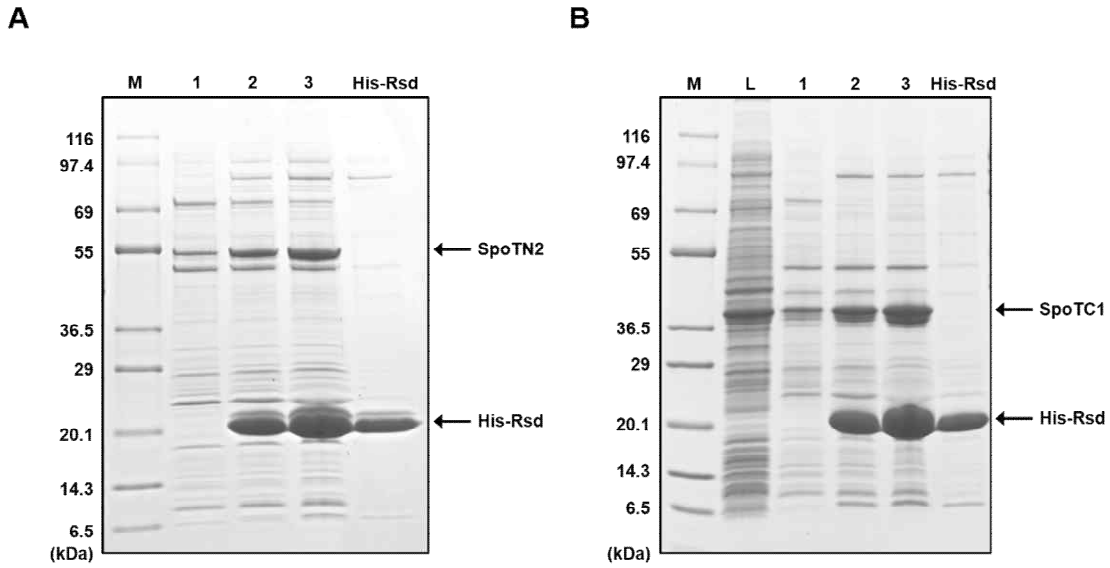

Fig. S2. Direct interaction of Rsd with the TGS domain of SpoT. Two truncated forms of SpoT containing the TGS domain, SpoTN2 (*A*) and SpoTC1 (*B*), were expressed in *E. coli*, and crude extracts were mixed with various amounts of purified His-Rsd (0, 120, and 360 μg in lanes 1-3, respectively). Each mixture was incubated with 50 μl TALON resin for metal affinity chromatography. Bound proteins were eluted with 70 μl of 2x SDS sample buffer and analyzed by SDS-PAGE and Coomassie blue staining. Purified His-Rsd was run as a control. Lane M, the molecular mass markers (KOMA Biotech); lane L in panel *B*, the crude cell lysate loaded on the TALON resin.

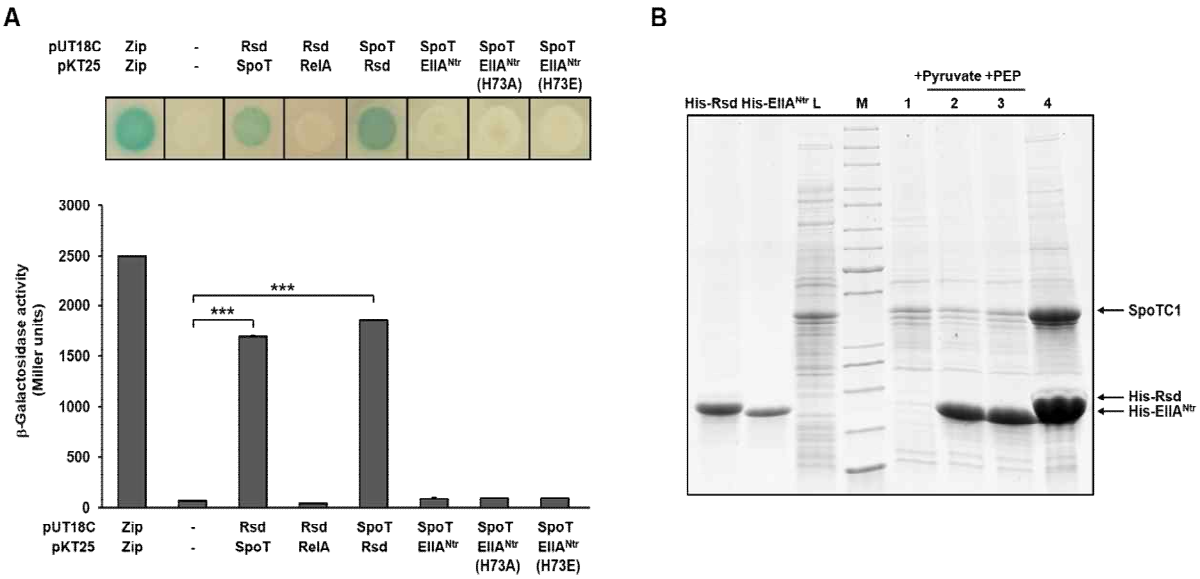

Fig. S3. Specific interaction of Rsd with SpoT. (*A*) *E. coli* strain BTH101 coexpressing the indicated fusion proteins was spotted on LB agar plates supplemented with 40 μg/ml X-gal as the color indicator for β-galactosidase activity and incubated at 30°C overnight. β-Galactosidase activity was measured in strains coexpressing indicated proteins by direct enzyme assay (Miller units). Zip, the leucine zipper domain of *S. cerevisiae* GCN4, served as a positive control. The transformant coexpressing the unfused T25- and T18-fragments served as a negative control. The mean and standard deviation (SD) of three independent measurements are shown. Statistical significance was determined using Student's t-test (***, $P < 0.001$). (*B*) An *E. coli* extract expressing SpoTC1 was mixed with binding buffer (lane 1), 300 μg of purified His-EIIA^{Ntr} in the presence of 1 mM pyruvate (lane 2) or 1 mM PEP (lane 3), and 300 μg of purified His-Rsd (lane 4). Each mixture was incubated with 50 μl of TALON resin for metal affinity chromatography. Proteins bound to the resin were eluted with 2x SDS loading buffer (70 μl) and analyzed by SDS-PAGE and stained with Coomassie brilliant blue. Lane L, the *E. coli* extract expressing SpoTC1; lane M, the molecular mass markers (Thermo Fisher Scientific).

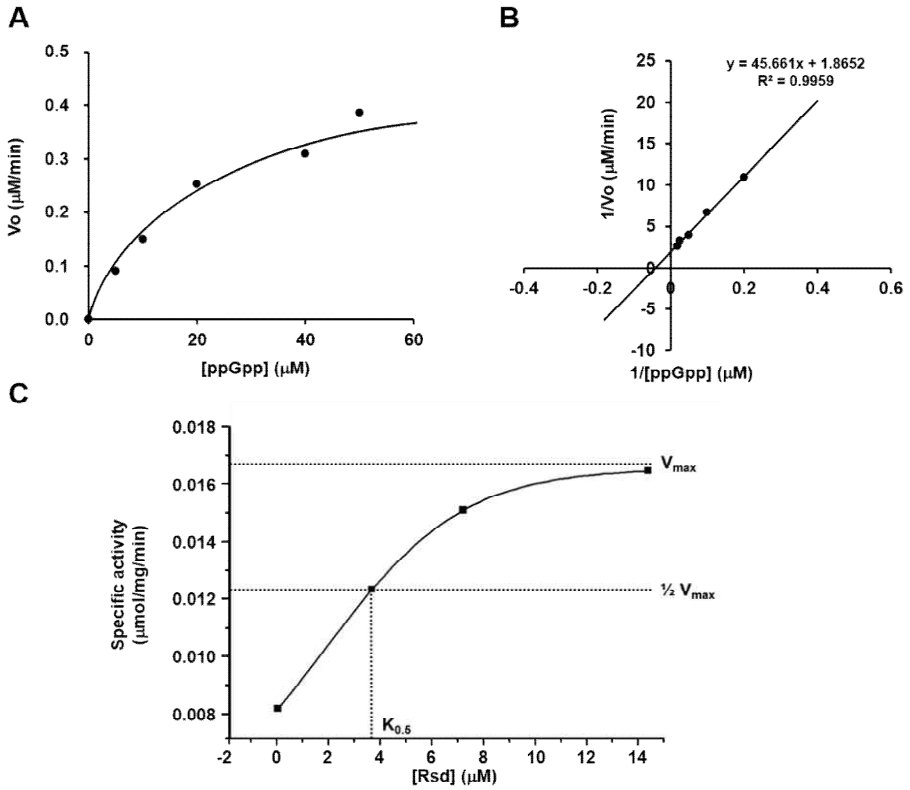

Fig. S4. Kinetic characterization of SpoT ppGpp hydrolase activity. (*A*) The ppGpp hydrolase activity of purified GST-SpoT (0.4 μM) was assayed in reaction mixtures containing various amounts of ppGpp. After incubation at 37°C for 7 min, reactions were stopped by the addition of formic acid to ~ 3%, then trifluoroacetic acid was added to a final concentration of 10%. The reaction products were analyzed by HPLC as described in *Materials and Methods*. The initial velocity of ppGpp hydrolysis (or GDP production) was plotted as a function of ppGpp concentration. Representative data from two independent experiments are shown. The data were fitted to Michaelis-Menten kinetics. (*B*) A Lineweaver-Burk plot of the data in panel *A*. (*C*) Concentration-dependent stimulation of the ppGpp hydrolase activity of SpoT by Rsd. The ppGpp hydrolase activity of purified GST-SpoT (0.4 μM) was assayed in reaction mixtures containing 30 μM ppGpp and various amounts of purified Rsd (0, 3.7, 7.3, and 14.6 μM). Reactions were processed and analyzed as described in panel *A*. Non-linear regression fits of experimental data were performed using Origin software. The concentration of Rsd required for half-maximum stimulation of the ppGpp hydrolase activity ($K_{0.5}$) was 3.65 μM. Representative data from two independent experiments are shown.

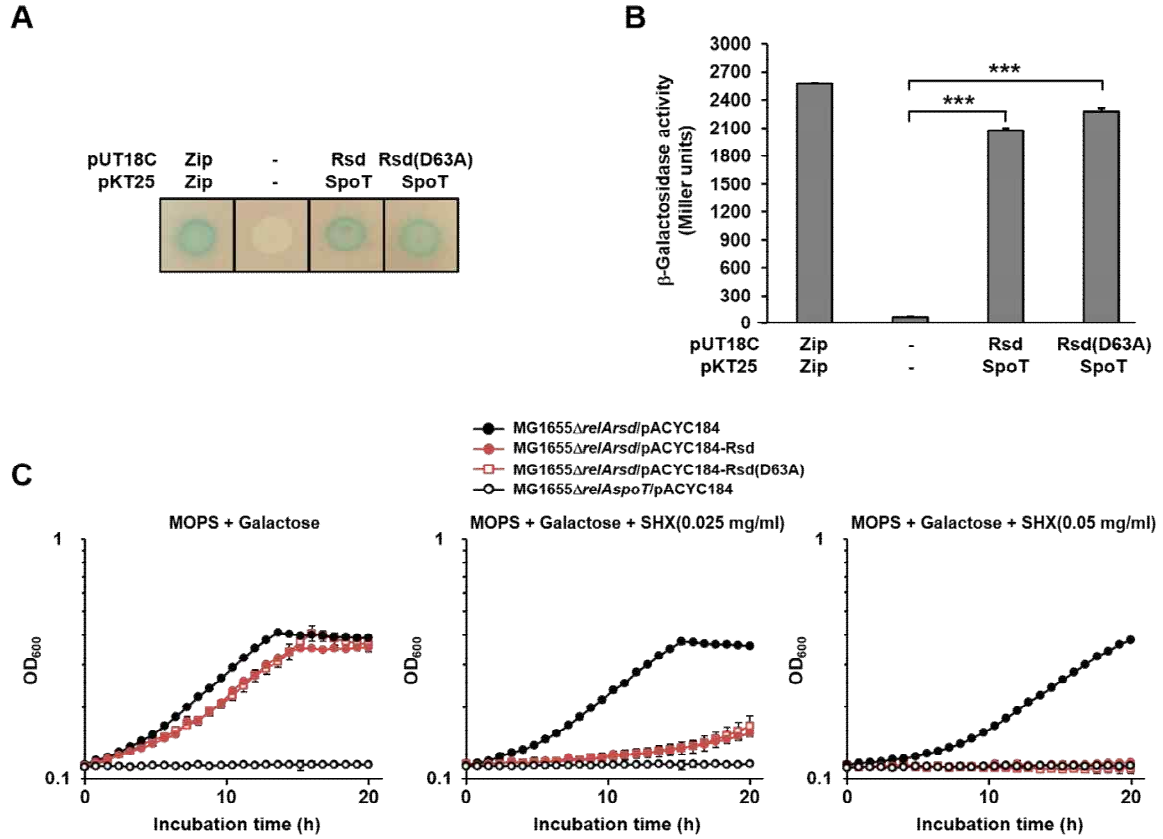

Fig. S5. Complex formation with SpoT and activation of the (p)ppGpp hydrolase activity of SpoT are independent of the anti-σ^{70} activity of Rsd. (*A* and *B*) The bacterial two-hybrid assays to analyze the specific interaction of Rsd and Rsd(D63A) with SpoT *in vivo*. *E. coli* BTH101 coexpressing T25-SpoT and T18-Rsd or T18-Rsd(D63A) was spotted on LB plates supplemented with 40 μg/ml X-gal (*A*) and β-galactosidase activity was monitored by direct enzyme assay (Miller units) (*B*). Zip served as a positive control. The transformant coexpressing the unfused T25- and T18-fragments served as a negative control. The mean and standard deviation (SD) of three independent measurements are shown. Statistical significance was determined using Student's t-test (***, $P < 0.001$). (*C*) Growth curves of *E. coli* strains in MOPS minimal medium (pH 7.2) supplemented with 0.2% galactose with or without SHX. After inoculation, 100-μl aliquots of each strain were transferred into a 96-well plate and growth was monitored at 600 nm using a multimode microplate reader (TECAN). The mean and standard deviation (SD) of three measurements are shown.

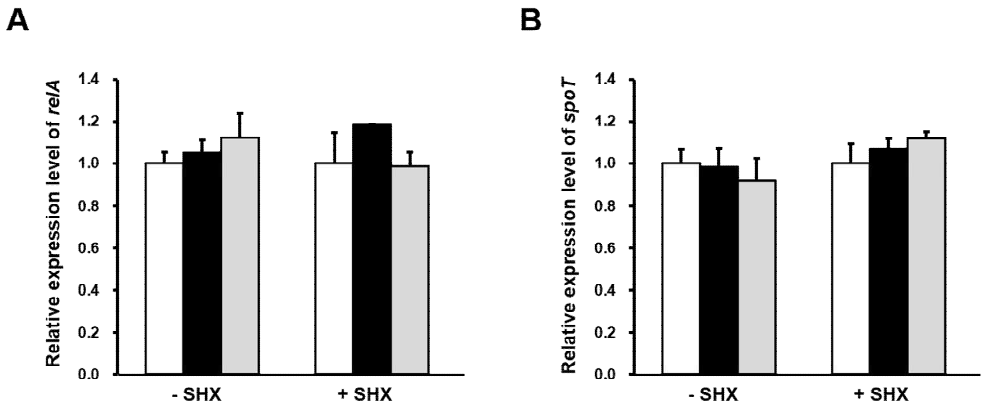

Fig. S6. The effect of Rsd on the transcription of *relA* and *spoT*. (*A* and *B*) The relative transcript levels of *relA* (*A*) and *spoT* (*B*) were determined by quantitative reverse transcriptase PCR (qRT-PCR). *E. coli* cells were grown in LB medium containing appropriate antibiotics and 0.02% arabinose. At OD_{600} ~0.6, each culture was divided into two parts and SHX (0.5 mg/ml) was added to one of them. After 30-min incubation, cells were harvested and total RNA was prepared using MiniBEST Universal RNA Extraction Kit (Takara Bio). Genomic DNA was removed using RNase-free DNase I (Promega). The same amount of RNA (2500 ng) from each culture was converted into cDNA using cDNA EcoDry™ Premix (Takara Bio). cDNAs were diluted 20-fold and subjected to qRT-PCR analyses using gene-specific primers and SYBR Premix Ex Taq II (Takara Bio). Amplification and detection of specific products were performed using the CFX96 Real-Time System (Bio-Rad). For normalization of the transcript level, the *rrsG* gene was used as a reference. The relative expression level was calculated as the difference between the threshold cycle (Ct) of the target gene and the Ct of the reference gene for each template. The mean and standard deviation (SD) of three independent measurements are shown. MG1655/pJK1113, white; MG1655Δ*rsd*/pJK1113, black; MG1655Δ*rsd*/pJK1113-Rsd, gray.

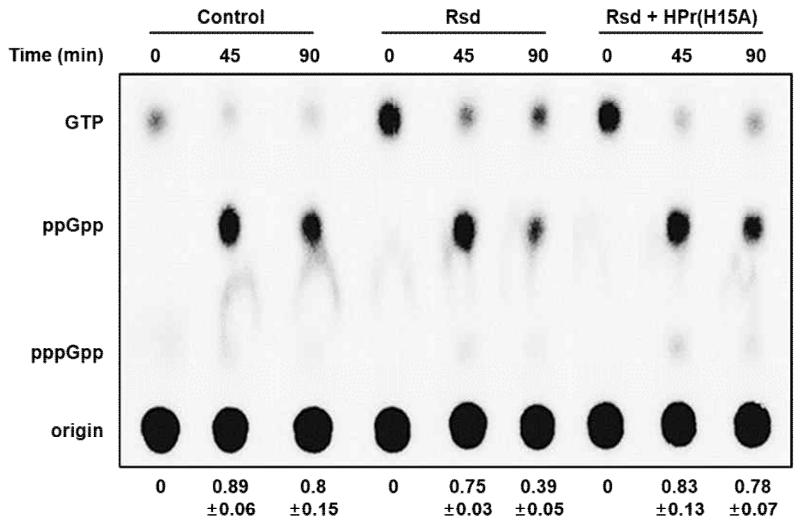

Fig. S7. Dephosphorylated form of HPr abolishes the stimulatory effect of Rsd on the (p)ppGpp hydrolase activity of SpoT. The MG1655Δ*rsd* strain carrying pJK1113 (Control), pJK1113-Rsd (Rsd), or both pJK1113-Rsd and pJK1113-H15A (Rsd + HPr(H15A)) was incubated in low-phosphate MOPS minimal medium containing 0.2% galactose and 0.02% arabinose and 100 μCi/ml $^{32}PO_4^{3-}$. Exponentially growing cells were treated with SHX (1 mg/ml) and intracellular (p)ppGpp concentrations were analyzed by TLC at three time points (indicated above each lane). Relative amounts of (p)ppGpp were calculated as the intensity of (p)ppGpp divided by that of (p)ppGpp plus GTP. The mean and standard deviation (SD) of three independent measurements are shown below each lane.

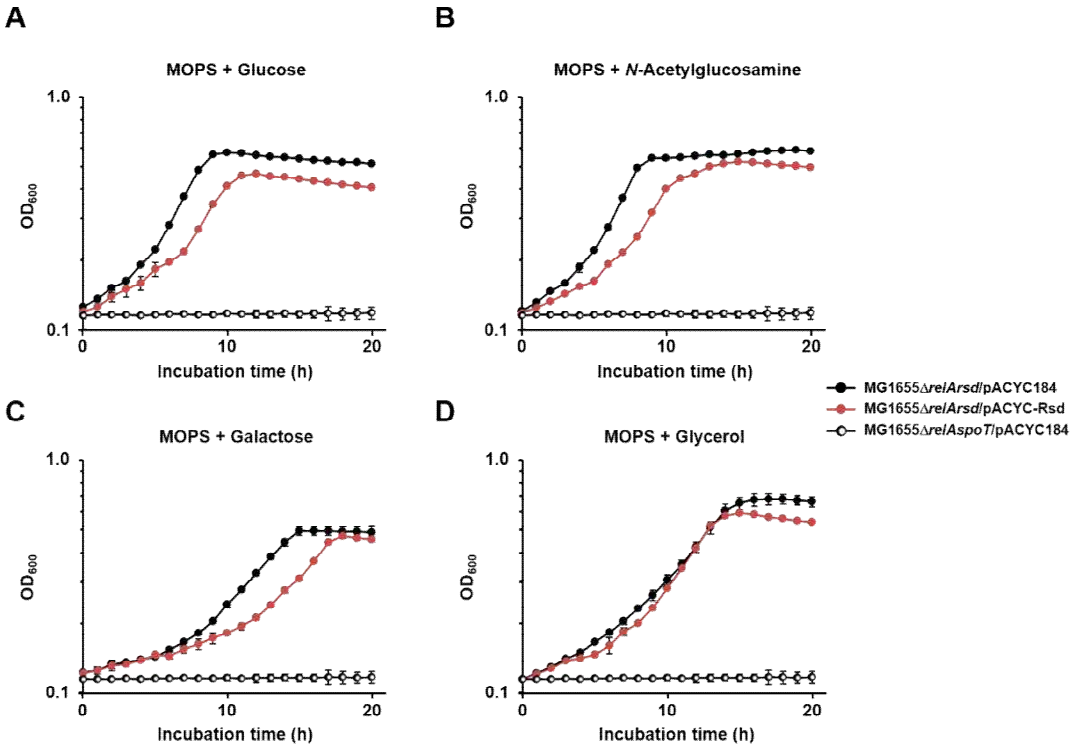

Fig. S8. Growth curves of *E. coli* strains in MOPS minimal medium containing different carbon sources. Each strain was inoculated in MOPS minimal medium (pH 7.2) supplemented with 0.2% glucose (*A*), *N*-acetylglucosamine (*B*), galactose (*C*), or glycerol (*D*). After inoculation, 100-µl aliquots of each strain were transferred into a 96-well plate and growth was monitored at 37°C by measuring the OD_{600} in multimode microplate reader (TECAN). The mean and standard deviation (SD) of three measurements are shown.

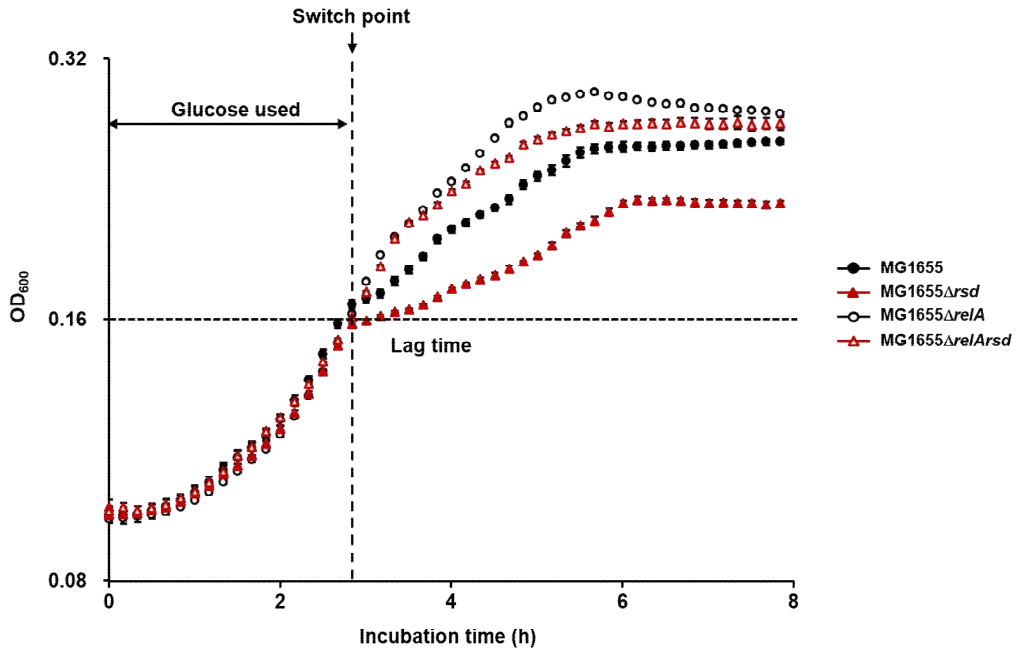

Fig. S9. Rsd is required to counterbalance RelA-mediated (p)ppGpp accumulation during a carbon source downshift. *E. coli* strains grown overnight in LB medium were harvested, washed, and then suspended in MOPS minimal medium containing 0.1% casamino acids and 0.02% glucose. After inoculation, 100-µl aliquots of each strain were transferred into a 96-well plate and growth was monitored at 600 nm using a multimode microplate reader (TECAN). The mean and standard deviation (SD) of three measurements are shown.

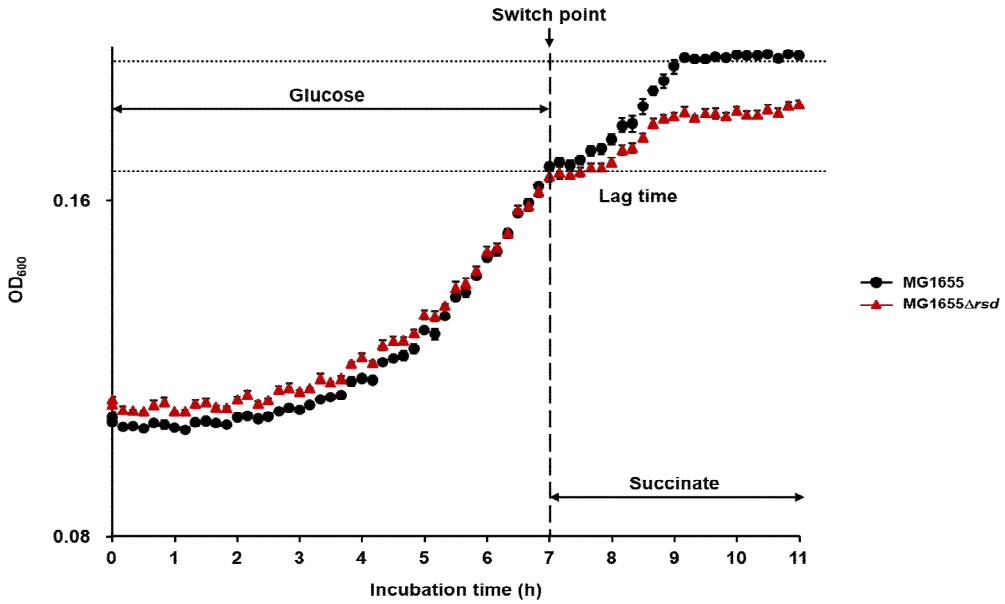

Fig. S10. Rsd is involved in the response to a carbon source downshift. *E. coli* strains grown overnight in LB medium were harvested, washed, and then suspended in MOPS minimal medium containing 0.04% glucose and 0.08% succinate. After inoculation, 100-µl aliquots of each strain were transferred into a 96-well plate and growth was monitored at 600 nm using a multimode microplate reader (TECAN). The mean and standard deviation (SD) of three measurements are shown.

Supplementary References

1. Blattner FR, *et al.* (1997) The complete genome sequence of *Escherichia coli* K-12. *Science* 277(5331):1453-1462.
2. Karimova G, Ullmann A, & Ladant D (2000) A bacterial two-hybrid system that exploits a cAMP signaling cascade in *Escherichia coli*. *Methods Enzymol* 328:59-73.
3. Park YH, Lee CR, Choe M, & Seok YJ (2013) HPr antagonizes the anti-σ^{70} activity of Rsd in *Escherichia coli*. *Proc Natl Acad Sci U S A* 110(52):21142-21147.
4. LaVallie ER, *et al.* (1993) A thioredoxin gene fusion expression system that circumvents inclusion body formation in the *E. coli* cytoplasm. *Biotechnology (N Y)* 11(2):187-193.
5. Karimova G, Pidoux J, Ullmann A, & Ladant D (1998) A bacterial two-hybrid system based on a reconstituted signal transduction pathway. *Proc Natl Acad Sci U S A* 95(10):5752-5756.
6. Karimova G, Ullmann A, & Ladant D (2001) Protein-protein interaction between *Bacillus stearothermophilus* tyrosyl-tRNA synthetase subdomains revealed by a bacterial two-hybrid system. *J Mol Microbiol Biotechnol* 3(1):73-82.
7. Karimova G, Dautin N, & Ladant D (2005) Interaction network among *Escherichia coli* membrane proteins involved in cell division as revealed by bacterial two-hybrid analysis. *J Bacteriol* 187(7):2233-2243.
8. Park S, Park YH, Lee CR, Kim YR, & Seok YJ (2016) Glucose induces delocalization of a flagellar biosynthesis protein from the flagellated pole. *Mol Microbiol* 101(5):795-808.

9. Datsenko KA & Wanner BL (2000) One-step inactivation of chromosomal genes in *Escherichia coli* K-12 using PCR products. *Proc Natl Acad Sci U S A* 97(12):6640-6645.

10. Reddy P, Peterkofsky A, & McKenney K (1989) Hyperexpression and purification of *Escherichia coli* adenylate cyclase using a vector designed for expression of lethal gene products. *Nucleic Acids Res* 17(24):10473-10488.

11. Lee CR*, et al.* (2005) Requirement of the dephospho-form of enzyme IIA^{Ntr} for derepression of *Escherichia coli* K-12 *ilvBN* expression. *Mol Microbiol* 58(1):334-344.

12. Choe M, Park YH, Lee CR, Kim YR, & Seok YJ (2017) The general PTS component HPr determines the preference for glucose over mannitol. *Sci Rep* 7:43431.

13. Chang AC & Cohen SN (1978) Construction and characterization of amplifiable multicopy DNA cloning vehicles derived from the P15A cryptic miniplasmid. *J Bacteriol* 134(3):1141-1156.